Cluster Ion Formation in Electrosprays of Acetonitrile Seeded with Ionic Liquids

ARTICLE *in* THE JOURNAL OF PHYSICAL CHEMISTRY B · SEPTEMBER 2004

Impact Factor: 3.3 · DOI: 10.1021/jp0401933

2 AUTHORS:

Bon Ki Ku
Centers for Disease Control and Prevention
33 PUBLICATIONS **1,509** CITATIONS
SEE PROFILE

Juan Fernandez de la Mora
Yale University
168 PUBLICATIONS **4,846** CITATIONS
SEE PROFILE

Cluster Ion Formation in Electrosprays of Acetonitrile Seeded with Ionic Liquids

Bon Ki Ku and Juan Fernandez de la Mora*

Yale University, Mechanical Engineering Department, New Haven, Connecticut 06511

Received: February 27, 2004; In Final Form: July 7, 2004

Clusters formed in positive electrosprays of several room-temperature molten salts A^+B^- dissolved (~1 mM) in acetonitrile are investigated in their natural charge state by high resolution differential mobility analysis. They exhibit a peculiar pattern of singly and doubly charged cluster ions $(A^+)_z(AB)_n$. For $z = 1$, there is a first series of clusters with n values typically from 0 to 3, peaking at about $n = 1$, and a second series with n values up to 8−12, peaking at about $n = 6$. Doubly charged clusters exhibit also two well-separated groups of ions. The two distinct series observed are attributed to two different ionization mechanisms, the small clusters forming by ion evaporation, and the large ones as charged residues from evaporating drops. The new ability to distinguish ions formed by either scheme provides information on the ranges of cluster sizes that may ion evaporate. Noteworthy is the observation that clusters grouping two cations do evaporate directly from the liquid surface.

1. Introduction

Electrospray is a widely used technique for producing gas phase ions, including multiply charged ions, from dilute species in solution.[1] Although not often used in this mode, when the sprayed species are relatively concentrated in solution, electrospray is also a very effective source of cluster ions.[2,3] The production of such clusters has been exploited for a variety of purposes, including high mass calibrants for mass spectrometry [4] or mobility spectrometry,[5] studies on the ionization mechanism in electrospray (ESI),[6,7] etc. Among the later studies, the relation between cluster size and charge has been used to identify the largest and smallest cluster capable of existing with a given number of elementary charges z. On the assumption that these critical sizes are due to the mechanism of charge loss by ion evaporation, several studies have made inferences on the kinetics of ion evaporation and not only concluded that the Iribarne−Thomson mechanism[8] is generally correct, but have also managed in a few ion−solvent combinations to determine the two basic parameters governing the ionization kinetics.[7] The prevailing picture today is that small ions are produced by the ion evaporation mechanism.[9] In contrast, many large ions seem to be unable to evaporate from a liquid surface and, hence, must remain trapped in the original charged drop (or one of its many daughters produced by a chain of Coulomb explosions) until it dries completely, leaving as a solid charged residue all the involatile material previously dissolved in the drop. This is Dole's well-known "charged residue mechanism".[10] When the initial solution is sufficiently dilute for this residue to contain just one molecule, the ion products from the two mechanisms are identical. The mechanisms themselves remain evidently different and are characterized by widely different ionization rates. But inferring which particular mechanism produces what particular ion is not straightforward.

The distinction is nonetheless possible under special circumstances. For instance, when the spraying Taylor cone is in a vacuum and drops have no chance to evaporate, it is evident that all ions and cluster ions observed must be produced by ion evaporation. There is an important body of literature in so-called electrohydrodynamic mass spectrometry (EHD-MS) exploiting this phenomenon, mostly based on glycerol electrolytes.[11] This approach has been recently extended to other polar solvents of low volatility (such as formamide;[12−14]) as well as to room-temperature molten salts,[15] often referred to as ionic liquids.[16] These studies have established firmly that small ions, either bare or clustered among themselves, and often attached to a varying number of solvent molecules, are ejected directly from the liquid surface into the vacuum. The simplest such situation studied is that of molten salts A^+B^-, where the solvent, the analyte, and the buffer ion are all the same thing. The pattern of ions observed must then be of the form $(A^+)_z(AB)_n$. In the ionic liquid ethyl−methyl imidazolium tetrafluoroborate ($EMIBF_4$), the dominant species seen are all singly charged, with $n = 0$ and 1, with small contributions of $n = 2$.[15] Worthy of note is the fact that this ionic liquid is sufficiently conducting to admit a spraying regime where most of the current comes in the form of ions, with little or no company of drops. Ion evaporation is therefore primarily directly from the liquid meniscus tip rather than from the drops.[12,15]

Despite their considerable interest, these vacuum techniques have not been successfully implemented with most common electrospray solvents (water, methanol, acetonitrile, etc.), which are too volatile to be electrosprayed into a vacuum. Hence, many ambiguities remain in relation to both mechanisms. For instance, although few doubt the importance of the ion evaporation mechanism for the production of small ions and cluster ions, we do not know how large an ion could be evaporated, or whether groupings of small ions containing several excess cations or anions can evaporate, and if so, up to what mass, or what charge level, or what is the evaporation pattern of size versus charge state, etc. Similarly, although Dole's mechanism is well established as the sole source of large compact multiply charged electrospray ions,[17] the possibility that long chains of industrial or biological polymers would, when spread out over the drop surface, also evaporate as ions remains open.[18] In view of these ambiguities, the purpose of this study is to use atmospheric pressure electrosprays to investigate the clustering pattern of a number of large salts dissolved in acetonitrile. Our aim is, in particular, to establish criteria to distinguish cluster

10.1021/jp0401933 CCC: $27.50
Published on Web 09/02/2004

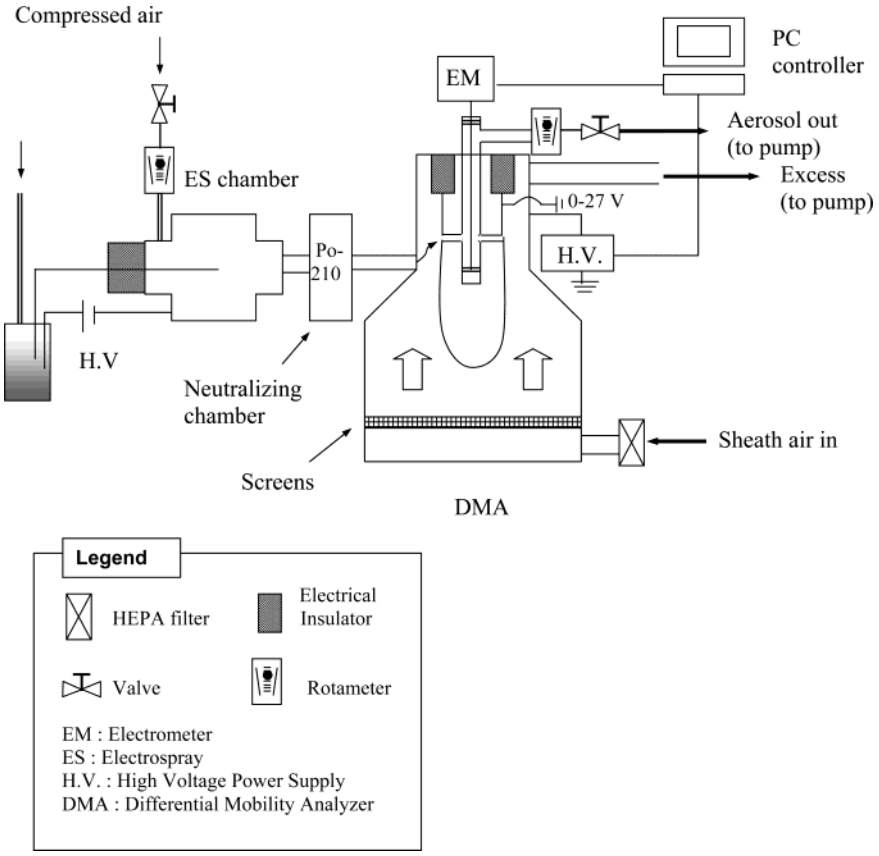

Figure 1. Experimental setup.

TABLE 1: Composition and Concentration of Various Salts Used in This Study

solution name[a]	composition	concn (mM)	mol wt
$EMIBF_4$	$(C_6H_{11}N_2)^+(BF_4)^-$	1	197.98
EMIIm	$(C_6H_{11}N_2)^+(N(SO_2CF_3)_2)^-$	1	391.32
EMIBeti	$(C_6H_{11}N_2)^+(N(SO_2CF_2CF_3)_2)^-$	1	491.36
DMPIMe	$(C_8H_{15}N_2)^+(C(SO_2CF_3)_3)^-$	1	550.44
TBAPOS	$(C_4H_9)_4N^+(F_{17}C_8O_3S)^-$	2	741.60

[a] Solution names are abbreviated for simplicity. EMI: 1-ethyl-3-methylimidazolium. DMPI: 1,2-dimethyl-3-propylimidazolium. BF_4: tetrafluoroborate. Im: bis(trifluoromethylsulfonyl)imide. Beti: bis(perfluoroethylsulfonyl)imide. Me: tris(trifluoromethylsulfonyl)methide. TBAPOS: Tetrabutylammonium perfluorooctanesulfonate.

ions formed by the two mechanisms, and to do so not only for singly charged clusters but also for those in higher charge states. All the salts chosen for this investigation are liquid at room temperature and are therefore susceptible to ion evaporation studies by mass spectrometry from a Taylor cone formed directly in a vacuum. Although partly complementary, the vacuum and atmospheric studies probe different things, because in one case the ions evaporate from their own molten salt, and in the other from an organic solvent.

2. Experimental Section

A schematic of the experimental setup is shown in Figure 1. Table 1 compiles information on the various salts (ionic liquids) used, including their names, abbreviation, chemical composition, and typical concentration in acetonitrile. Acetonitrile was purchased from J. T. Baker, TBAPOS and $EMIBF_4$ from Fluka, and EMIIm, EMIBeti, and DMPIMe from Covalent Associates (Woburn, MA). The liquid is pushed through a silica needle (20 μm i.d., 360 o.d.; Polymicro Technologies) by the controlled pressure difference between its reservoir (1 cm^3 polypropylene vial) and the sharpened end of the needle, held inside an electrospray chamber. The liquid tip is electrified through the solution in the vial, put in electrical contact with a high voltage power supply through a platinum electrode. Air is introduced in the electrospray chamber and drawn together with the dried electrospray residues and ions through a thin plate orifice into the analyzer. Three types of experiments were executed, depending on the device interposed between this thin-plate orifice and the inlet of the analyzer. Some auxiliary experiments aimed at distinguishing singly from multiply charged ions decreased the natural charge of the ions by inserting a charge-reduction (neutralizing) chamber, where a 5 mCurie ^{210}Po source (Model P-2042; NRD, Grand Island, NY) provides a bipolar ionic atmosphere that brings the charge level of the particles down to at most one elementary charge.[19] The level of charge reduction is controlled by partially blocking the active surface with a perforated plate. The charge reduction chamber was retained without its radioactive source in some experiments aimed at increasing the residence time of the ions prior to analysis, to help identify metastable species. A typical flow rate of the air gas is 2.5 L/min, the chamber volume is about 40 cm^3, with an associated time delay of about 1 s. This configuration will be referred to as *slow sampling*. In other experiments to be referred to as *fast sampling*, the ions were drawn directly from the electrospray chamber into the analyzer without such time delay and in their natural charge state. The sampling (either *fast* or *slow*) in the natural charge state will be referred to as *nonneutralized* whereas sampling with charge reduction based on the Po source will be referred to as *neutralized*. In all three cases, the ion-laden gas was then drawn through a short tube ($^1/_4$ in. o.d.) into the inlet port of a differential mobility analyzer (DMA). This instrument is based on the designs commonly used

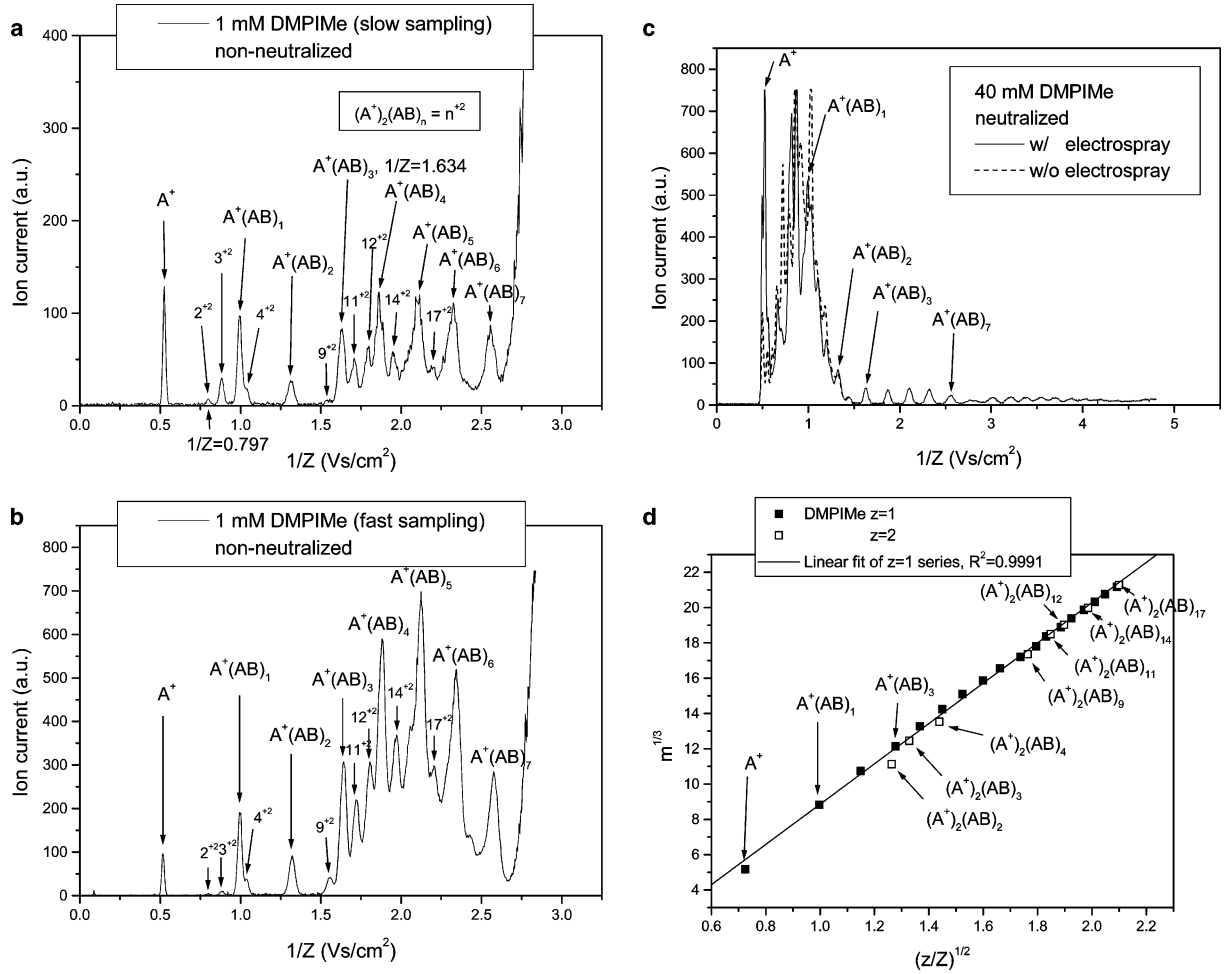

Figure 2. Mobility spectra for DMPIMe with naturally charged ions (no neutralization) and slow sampling (a) and naturally charged ions and fast sampling (b). Comparison of mobility spectra with and without electrospray for charge-reduced ions (c). Corresponding mass vs mobility data are shown in (d) for singly and doubly charged ions.

for particle sizing,[20] which separate a narrow range of particle mobilities out of an input flow including particles of many sizes and charges. DMAs combine the axial forced flow field and the radial electric field formed between two concentric cylinders to separate ions in space rather than in time. All ions enter through a narrow slit on the outer cylinder and are pushed downstream by the gas flow in the axial direction, and radially toward the inner electrode by the electric field. Only those ions with a narrow mobility range are sampled through another narrow slit on the inner cylinder. The prototype used in this work is of the Eichler type,[21,22] and has a full peak width at half-height (fwhh) of 2.2%. The mobility-selected ions are collected into a wire connected to an electrometer commercially supplied by Lazcano Inc. (joelaz@arrakis.es), with a response time of about 1 s and a noise level of about 10^{-16} ampere.

We calibrate the mobility of the clusters using as a standard the known mobility of the dimer ion $A^+(ABr)$ ($1/Z = 1.51$ (V s)/cm^2),[7a] where A^+ stands for the tetraheptylammonium cation. This ion is electrosprayed from a dilute (~1 mM) alcohol solution.

3. Results

3.1. Ion Assignment. Figure 2 shows several mobility spectra for DMPIMe, including peak assignments. One sees first a *discrete* region to the left, where individual peaks rise in isolation. Then follows a fairly crowded region between about 1.5 and 3 (V s)/cm^2, where a denser group of peaks rises above what appears as a *continuous* background. Our assignment of charge state z and state of aggregation n of the clusters $(A^+)_z(A^+B^-)_n$ will proceed without the assistance of a mass spectrometer and has been guided by several simple criteria. The apparently continuous background is in reality the superposition of numerous isolated peaks associated with relatively large multiply charged clusters. Their mobilities tend to lie in a restricted range because these clusters are formed as charged residues from dry electrospray drops evolving in the ion evaporation regime. As their solvent evaporates, these drops shed charge by ion evaporation and tend to evolve with a relatively constant surface electric field.[6] This makes their charge approximately proportional to the square of their diameter, keeping also their electrical mobility near a fixed value.[6] Earlier work based on a detector sensitive to the charge state[7a] or on a mass spectrometer [23] has seen that the discrete region contains only singly and doubly charged clusters ($z = 1, 2$), whereas charge states larger than 2 lie in the region of the continuous background. It is therefore safe to assume that z is either 1 or 2 for the isolated peaks observed. For greater confidence, singly charged ions have been identified independently by comparing naturally charged and charge-reduced mobility spectra, because, after charge reduction, singly charged ions remain in their original position in the spectrum, whereas multiply charged ions shift to lower mobilities. The simplification brought about by charge reduction comes at a cost, as the radioactive source ionizes air molecules and volatile impurities, which add to the

TABLE 2: Mass and Inverse Mobility of the Singly and Doubly Charged Ions Observed for Various Salts

	EMIBF4		EMIIm		EMIBeti		DMPIMe		TBAPOS	
ion	mass (amu)	$1/Z$ [(V s]/cm^2)	mass (amu)	$1/Z$ [(V s]/cm^2)	mass (amu)	$1/Z$ [(V s]/cm^2)	mass (amu)	$1/Z$ [(V s]/cm^2)	mass (amu)	$1/Z$ [(V s]/cm^2)
					$z = 1$					
A^+	111.168	0.495	111.168	0.489	111.168	0.493	139.22	0.525	242.46	0.711
$A^+(AB)$	309.148	0.861	502.488	0.847	602.528	0.858	689.66	0.992	984.06	1.366
$A^+(AB)_2$	507.128	1.080	893.808	1.095	1093.888	1.205	1240.1	1.322	1725.66	1.768
$A^+(AB)_3$	705.108	1.255	1285.128	1.326	1585.248	1.471	1790.54	1.634	2467.26	2.237
$A^+(AB)_4$	903.088	1.359	1676.448	1.549	2076.608	1.733	2340.98	1.868	3208.86	2.549
$A^+(AB)_5$	1101.068	1.471	2067.768	1.747	2567.968	1.967	2891.42	2.102	3950.46	2.928
$A^+(AB)_6$	1299.048	1.600	2459.088	1.932	3059.328	2.169	3441.86	2.322	4692.06	3.256
$A^+(AB)_7$	1497.028	1.704	2850.408	2.130	3550.688	2.378	3992.3	2.559	5433.66	3.558
$A^+(AB)_8$	1695.008	1.811	3241.728	2.283	4042.048	2.566	4542.74	2.761	6175.26	3.758
$A^+(AB)_9$	1892.988	1.926	3633.048	2.421	4533.408	2.747	5093.18	3.020	6916.86	4.044
$A^+(AB)_{10}$	2090.968	2.037	4024.368	2.563	5024.768	2.903	5643.62	3.222	7658.46	4.275
$A^+(AB)_{11}$	2288.948	2.131	4415.688	2.719	5516.128	3.062	6194.06	3.357	8400.06	4.572
$A^+(AB)_{12}$	2486.928	2.238	4807.008	2.846	6007.488	3.226	6744.5	3.559	9141.66	4.797
$A^+(AB)_{13}$	2684.908	2.335	5198.328	2.977	6498.848	3.357	7294.94	3.704	9883.26	4.971
$A^+(AB)_{14}$	2882.888	2.432					7845.38	3.885		
$A^+(AB)_{15}$	3080.868	2.547					8395.82	4.045		
$A^+(AB)_{16}$							8946.26	4.197		
$A^+(AB)_{17}$							9496.7	4.378		
					$z = 2$					
$(A^+)^2(AB)_2$			1004.976	0.656	1205.056	0.663	1379.32	0.797	1968.12	1.036
$(A^+)^2(AB)_3$	816.276	0.667	1396.296	0.762	1696.416	0.769	1929.76	0.883	2709.72	1.170
$(A^+)^2(AB)_4$	1014.256	0.742	1787.616		2187.776	0.911	2480.2	1.035	3451.32	
$(A^+)^2(AB)_5$	1212.236	0.782	2178.936	0.907	2679.136	1.007	3030.64		4192.92	
$(A^+)^2(AB)_6$	1410.216		2570.256	0.999	3170.496	1.134	3581.08		4934.52	
$(A^+)^2(AB)_7$	1608.196		2961.576		3661.856		4131.52		5676.12	
$(A^+)^2(AB)_8$	1806.176	0.933	3352.896	1.199	4153.216	1.304	4681.96		6417.72	2.015
$(A^+)^2(AB)_9$	2004.156		3744.216		4644.576	1.394	5232.4	1.556	7159.32	
$(A^+)^2(AB)_{10}$	2202.136	1.023	4135.536	1.319	5135.936		5782.84		7900.92	2.168
$(A^+)^2(AB)_{11}$	2400.116		4526.856		5627.296		6333.28	1.709	8642.52	
$(A^+)^2(AB)_{12}$	2598.096	1.142	4918.176	1.474	6118.656	1.651	6883.72	1.801	9384.12	2.421
$(A^+)^2(AB)_{13}$							7434.16		10125.72	
$(A^+)^2(AB)_{14}$							7984.6	1.973		
$(A^+)^2(AB)_{15}$							8535.04			
$(A^+)^2(AB)_{16}$							9085.48			
$(A^+)^2(AB)_{17}$							9635.92	2.204		

complexity of the charge-reduced spectrum. This increased complexity, however, is restricted to relatively high mobilities, as seen in Figure 2c, where one of the two curves shown was taken without electrospay and contains only ions from the polonium source. We can hence be sure of which ions are originally singly charged.

The assignment of n for $z = 1$ by mobility alone has caused some errors in the past [7a] as recently noted in a DMA-MS study.[23] The problem in ref 7a was that the charge state z was determined in a second instrument (a condensation nucleus counter, CNC) following the DMA, yet multiply charged metastable ions may loose one charge between the DMA and the CNC. This led in ref 7a to the interpretation of the smallest doubly charged ion (particularly unstable) as singly charged, which threw off by one unit the whole singly charged series of tetraheptylammonium following the bare cation. Such an incidence is avoided here by being aware of the possible presence of doubly charged ions in the discrete spectrum, and assigning z only as just discussed. Because the dominant peak from spectra of relatively large salts such as those studied here is always the bare cation A^+, with substantial currents of the dimer $A^+(A^+B^-)$ and often also the trimer $A^+(A^+B^-)_2$,[7a,24,23] the whole $z = 1$ series can then be constructed by merely counting from the dominant and most mobile ion, assigned $n = 0$.

Ions in the discrete region known not to be singly charged are provisionally presumed to correspond to $z = 2$. For their assignment to an aggregation state n, we compare twice their inverse mobility with the inverse mobility of singly charged ions as a function of their mass. For example, the smallest doubly charged ion seen in Figure 2a has an inverse mobility $1/Z = 0.797$ (V s)/cm^2, twice of which ($2/Z = 1.594$ (V s)/cm^2) closely matches the value for $A^+(A^+B^-)_3$ ($1/Z = 1.634$ (V s)/cm^2). This doubly charged ion can therefore be safely assigned to $(A^+)_2(A^+B^-)_2$, which in turn fixes the structure of the whole doubly charged series. In other words, because the mass of $A^+(A^+B^-)_3$ and $A^+{}_2(A^+B^-)_2$ for DMPIMe are 1790.54 and 1379.32 amu, respectively, the heavier ion ($A^+(A^+B^-)_3$) should have a slightly higher inverse mobility than the lighter one ($A^+{}_2(A^+B^-)_2$). This assignment can be confirmed more confidently by plotting the ion mass (from the assigned structure) as a function of z/Z for both charge states, as seen in Figure 2d. Mass versus mobility data are also collected in Table 2. For spherical and relatively large ions, whose cross section in air is not significantly modified from its geometric value by polarization effects, their electrical mobility Z is related to their charge state z, and diameter d_p through the expression

$$Z = 0.441 \frac{ze(kT/m_g)^{1/2}}{p(d_p + d_0)^2} \qquad (1)$$

based on Millikan's formula for spheres in the free molecular regime. p, T, m_g, e, and k are the pressure, temperature, molecular mass of the carrier gas, elementary charge, and Boltzmann constant. This expression accounts for the effect of

the finite diameter of the molecules of the surrounding gas (taken here to be $d_0 = 0.53$ nm;[25,22]) but ignores polarization effects. Because both $m^{1/3}$ ($\sim d_p$) and $(z/Z)^{1/2}$ are linear in particle diameter, the graph should be a straight line, and this is the reason behind the choice of axes in Figure 2d. In addition to their continuity, the linearity of the data adds further confidence to our assignment of n for doubly charged ions. Because doubly charged ions tend to have weaker signals than singly charged ions, not all their peaks can be distinguished against the background of singly charged species, leading to gaps in the doubly charged series. This is illustrated in the mobility region from 1.5 to 2.5 Vs/cm^2, where doubly charged clusters with $n = 10$, 13, 15, and 16 are missing due to interference with singly charged ions with $n = 3$, 4, and 5. These discrete gaps pose no serious problem to series reconstruction, as seen in the m vs z/Z curve of Figure 2d. Of greater concern is the complete absence of doubly charged ions in the wide interval from $n = 5$ to $n = 8$, which weakens slightly the confidence on the n assignments for the clusters with $n < 5$, for which polarization effects may not be negligible. Given the large amount of multiply charged ions present in the crowded region between 1.5 and 3 (V s)/cm^2, the possibility exists that some of the sharp ion peaks, which are not singly charged, might have 3 rather than 2 charges. We have hence searched for triply charged ions following the same pattern used for $z = 2$ and reached the conclusion that none of the peaks interpreted as doubly charged can be charged otherwise.

We have also attempted a direct confirmation of the assignment of the isolated peaks interpreted as doubly charged directly by passing them to a mass spectrometer after selection with the DMA. Unfortunately, they are metastable and do not survive the transit from the atmospheric pressure source to the vacuum system of our mass spectrometer. However, a mobility-mass spectrometry investigation of tetraheptylammonium bromide clusters has identified distinct mass peaks at m/z values associated to doubly charged ions $(AB)_n(A^+)_2$ for $n = 7-11$.[23] Earlier work based on slight charge reduction of multiply charged tetraheptylammonium bromide clusters did form the complete set of stable doubly charged ions, which was analyzed by mobility alone (unambiguous charge assignment based on critical supersaturation for ion-induced nucleation).[7a] The n assignment is also unambiguous above 7,[23] and strongly supported by the principle of continuity down to $n = 3$. Continuity also permits the assignment of the metastable ion at $n = 2$.[23] This confirms for the tetraheptylammonium clusters all the general features used here (without mass analysis) to support the assignment of the $z = 2$ series.

Although we are confident that the (z, n) assignment made is correct, we note that, provided the assignment of z is right, most of the mechanistically important points to be made below are in fact independent of slight misassignments of n that may have crept into the $z = 2$ series.

3.2. Double Hump Structure of the Mobility Distributions. Note the following key qualitative features of the mobility spectra of DMPIMe:

(i) The discrete portion of the spectrum for singly charged ions consists of high mobility peaks with intensities reaching a maximum between $n = 0$ and $n = 1$, and decaying rapidly thereafter. The doubly charged members of the discrete spectrum share the same clear feature of reaching a maximum intensity at a certain n (3 or 4 in the case of DMPIMe), and decaying rapidly to zero to its right and left.

(ii) The singly and doubly charged ion peaks appearing over the continuum background between 1.5 and 2.5 (V s)/cm^2 do similarly attain a maximum intensity at about the middle of this interval decaying both to its right and to its left.

(iii) There is a gap between the two features just discussed (from 4^{+2} and 9^{+2}) where doubly charged ions are completely absent, even though much of the mobility range between both is free from interfering singly charged ions. The doubly charged clusters 5^{+2} and 6^{+2} are not produced at any measurable rate. The missing clusters 7^{+2} and 8^{+2} would fall on the left and right tail of $A^+(AB)_2$, though with sufficiently different mobilities to be distinguishable even at intensities 5−10 times smaller than that of $A^+(AB)_2$. The singly charged series shows a substantial intensity reduction in this gap region, but the ion signal does not fall to zero.

The simplest (though perhaps not the only possible) explanation for the observed presence of two separate series of ions is that each of them is produced by a different ionization mechanism. This behavior is exactly as one would have expected, given that the small singly charged clusters are known to be generally produced by ion evaporation, and the larger multiply charged clusters through the charged residue mechanism. In addition, our data show two new things: First, there is a measurable upper and a lower mass limit for ion evaporation, with a most favorable mass between, both for singly and doubly charged ions. The same may well happen for higher charge states, but mobility analysis is unable to distinguish the two corresponding series. A second conclusion is that the Iribarne−Thomson mechanism is capable of forming ion clusters grouping more than one cation. We shall later argue on the basis of Born's capillary model that these observations are qualitatively predictable from the ion evaporation theory itself.

The peculiar doubly humped pattern found in the naturally charged mobility spectra of DMPIMe applies similarly to all the salts examined, as shown in the spectra of Figures 3−6. This pattern has not been recognized in previous studies of tetraheptylammonium bromide clusters,[6a,23] whose singly charged series does not show two distinct features. Complete suppression of small charge residue formation was nonetheless attained in ref 7a, from which it was argued that ion evaporation takes place up to the cluster $A^+(AB)_4$ [which was taken to be $A^+(AB)_5$], with a mass of 2368 amu. Perhaps the lack of separation between the ion evaporated and residue humps was due in that case to the unusually high value of this upper mass, probably associated with the fact that tetraheptylammonium bromide is surface active, and relatively large clusters (micelles) must preexist in solution. We have reexamined the mobility spectra of electrosprays from tetraheptylammonium bromide and confirmed the existence of an isolated series of high mobility metastable doubly charged clusters, which must also be formed by ion evaporation.

We note finally that TBAPOS does not show as cleanly as the other samples the dome shape in the inverse mobility range from 1.5 to 3.0 (V s)/cm^2, perhaps due to the singularly large mass of this salt. Nonetheless, its mobility spectra still present a clear double hump distribution for both the singly and the doubly charged ions.

Several other interesting points can be drawn from Figures 2−6. Note, for instance, that, for DMPIMe, there is no substantial difference between fast and slow sampling spectra, except that the ions interpreted as charged residues are relatively more abundant under fast sampling. Had the most mobile doubly charged ions been metastable (as they are in the case of tetraheptylammonium),[7a,23] their relative contribution with respect to the singly charged ions would have increased considerably upon fast sampling. The smallest doubly charged DMPIMe clusters produced by electrospray are therefore relatively stable.

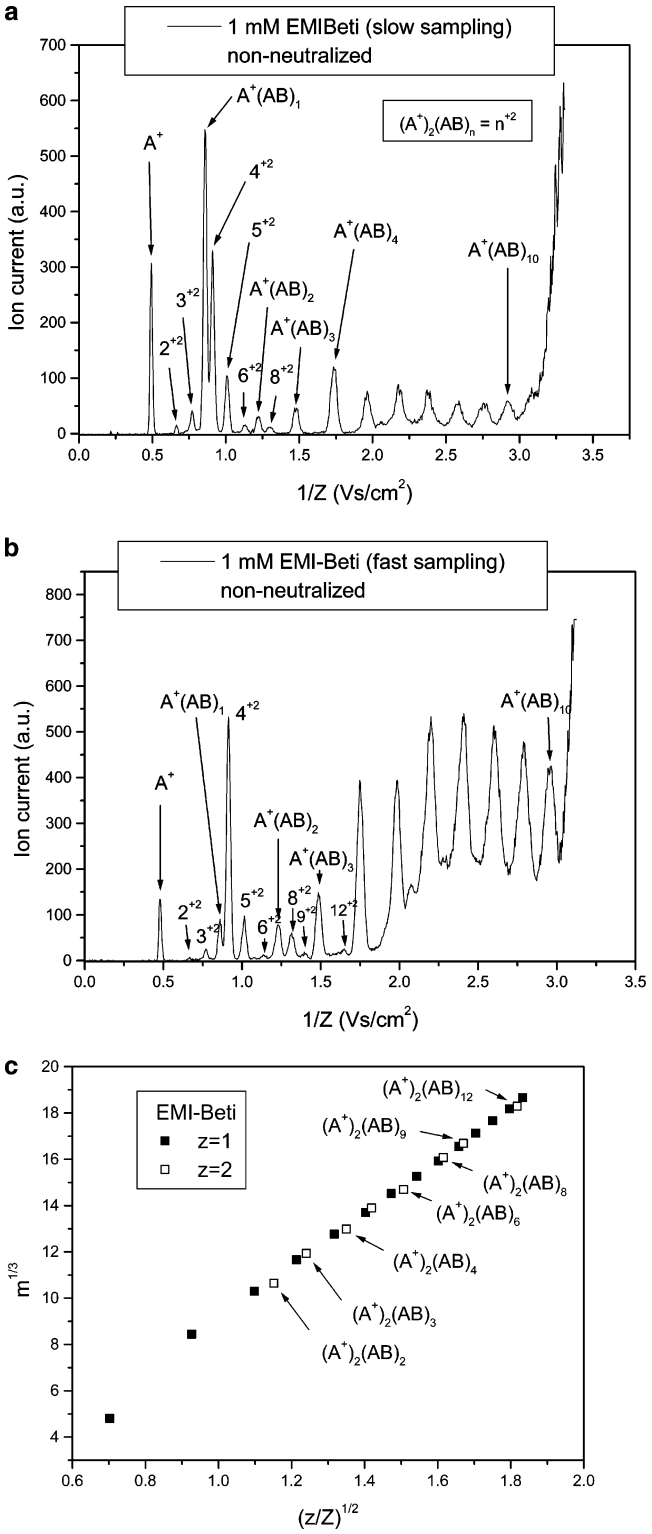

Figure 3. Mobility spectra of naturally charged ions (no neutralization) for EMIBeti with slow sampling (a) and fast sampling (b). The corresponding mass vs mobility data are shown in (c) for singly and doubly charged ions.

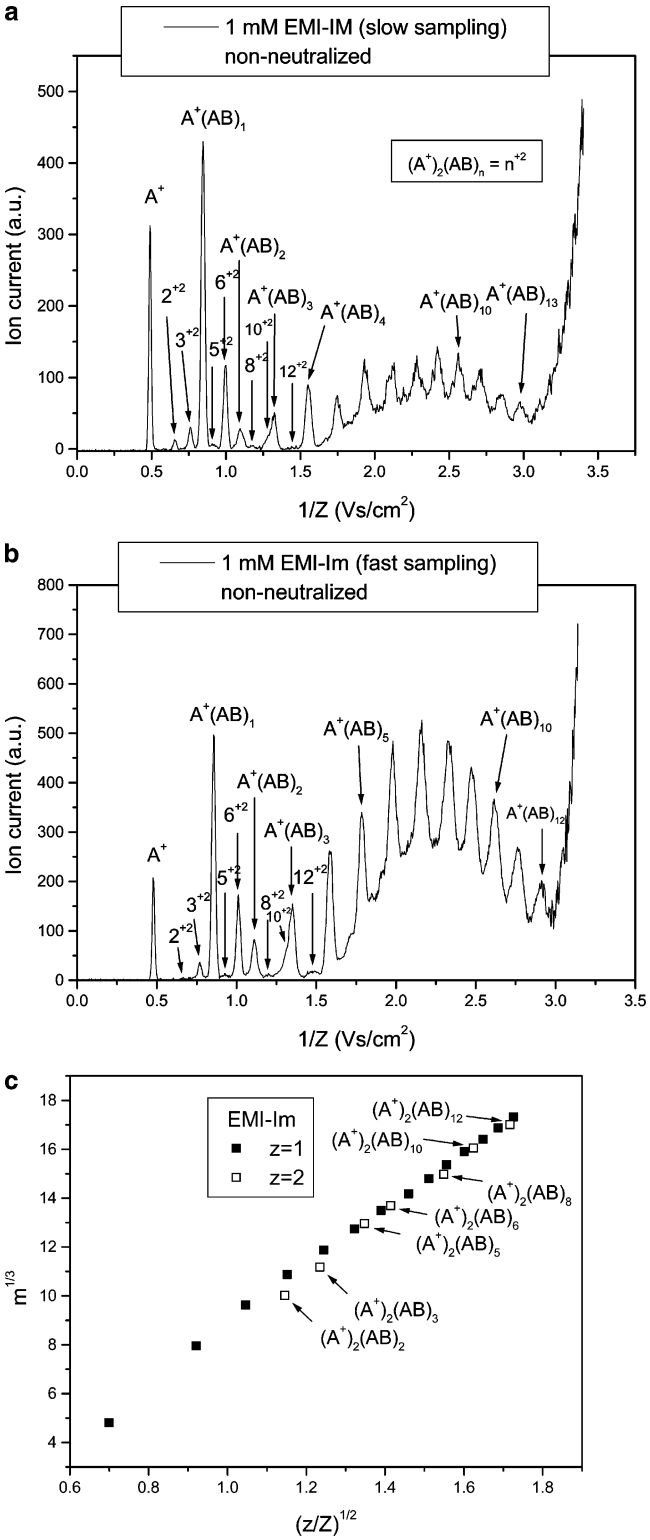

Figure 4. Mobility spectra of naturally charged ions (no neutralization) for EMIIm with slow sampling (a) and fast sampling (b). The corresponding mass vs mobility data are shown in (c) for singly and doubly charged ions.

The same holds for EMIBeti and EMIIm. In contrast, rapid sampling of the electrosprays from the smallest salt ($EMIBF_4$) clearly favors the signal of the smallest doubly charged ions, hinting at their instability.

3.3. Effect of the Electrospray Current. Parts a−c of Figure 7 show mobility spectra for EMIIm, EMIBeti, and DMPIMe. Each figure contains curves for several values of the liquid flow rate q_l fed into the electrospray needle, including the minimum flow rate below which the Taylor cone becomes unstable. All the spectra have been obtained with a fixed aerosol flow, 2.5 L/min, all variables but q_l remaining constant. q_l was not directly measured but is known to be proportional to the square of the spray current I, indicated in the labels.[26] Interestingly, the series of peaks we have associated with ion evaporation are almost unaffected by q_l, whereas the abundance of those attributed to Dole's mechanism increases substantially with it. This observa-

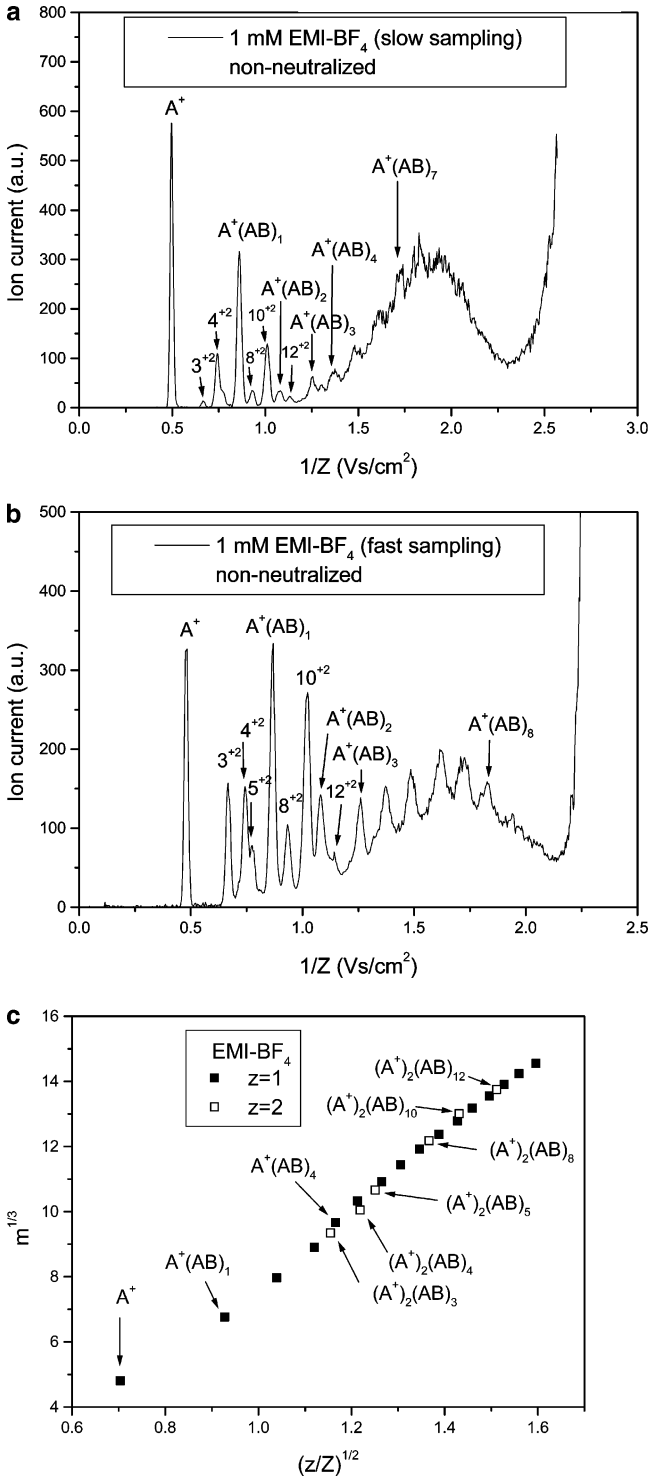

Figure 5. Mobility spectra of naturally charged ions (no neutralization) for $EMIBF_4$ with slow sampling (a) and fast sampling (b). The corresponding mass vs mobility data are shown in (c) for singly and doubly charged ions.

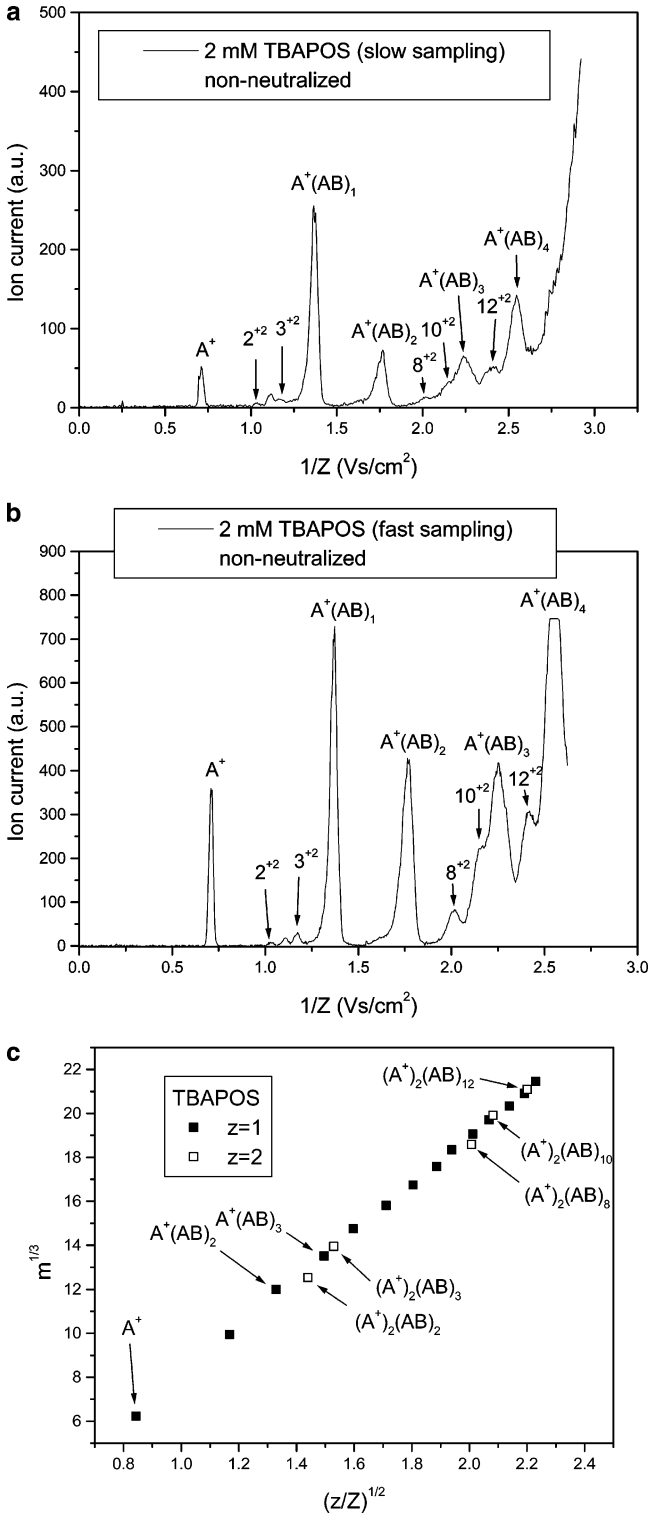

Figure 6. Mobility spectra of naturally charged ions (no neutralization) for TBAPOS with slow sampling (a) and fast sampling (b). The corresponding mass vs mobility data are shown in (c) for singly and doubly charged ions.

tion alone lends strong independent support to the notion that the two kinds of ions are formed by drastically different mechanisms. It would nonetheless be difficult to explain quantitatively the singular observation embodied in Figure 7 or draw from them more direct support for the claim that one of the humps is due to ion evaporation and the other to the charged residue mechanism.

3.4. Peak Width and Ionization Mechanism. We note another qualitative feature reinforcing the interpretation given to the two mobility modes observed. Ions evaporated directly from the drops would tend to be free from other impurities and hence produce sharp peaks associated to pure species. On the other hand, ions formed as charged residues would be attached to other involatile materials carried by the drop releasing them. Ions so produced would hence tend to be contaminated and produce wider envelope peaks rather than sharp mobility peaks. This trend has been previously reported for the case of tetraheptylammonium bromide clusters.[23] Visual examination of the mobility spectra in Figures 2−6 does indeed give the

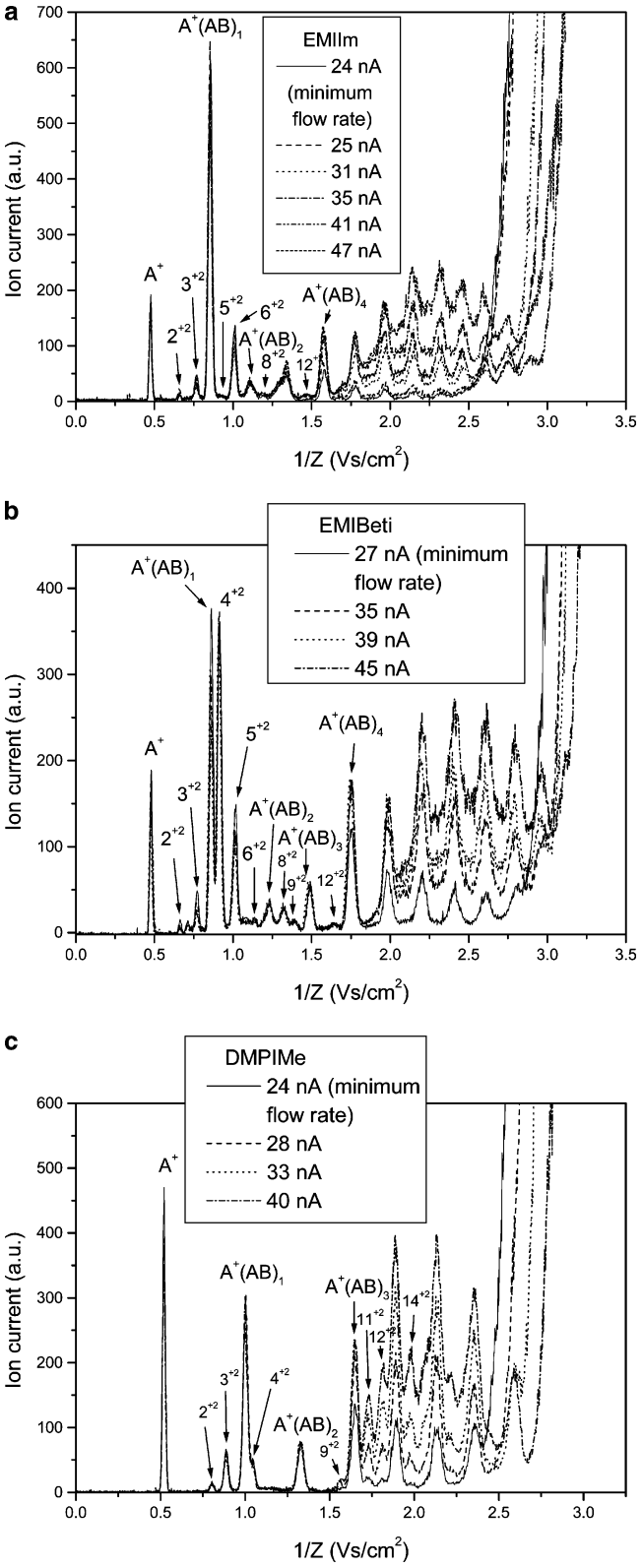

Figure 7. Mobility spectra of naturally charged ions at various liquid flow rates for solutions of EMIIm (a), EMIBeti (b), and DMPIMe (c).

qualitative impression that the peaks to the right are substantially wider than those to the left. This trend, however, is difficult to support quantitatively, because the presence of background below the less mobile peaks introduces a large ambiguity in the definition of their width. Still, we note for example, that the full width at half-height (fwhh) in Figure 3 is 0.0316 for $(A^+)_2(A^+B^-)_4$ (4^{+2}), which is almost identical to the value for 1^+. This fact together with the high intensity of this doubly charged peak indicates strongly that 4^{+2} is produced by ion evaporation

TABLE 3: Radius for Maximum Peak Height of $z = 1$ and $z = 2$

z (nm)	DMPIMe	EMIBeti	EMIIm	$EMIBF_4$	TBAPOS
1	0.44	0.39	0.39	0.39	0.57
2	0.76	0.69	0.74	0.75	0.82

3.5. Ion Evaporation Probability versus Mass and Charge. Further qualitative support for the hypothesis that the singly and doubly charged ions contained in the first mobility hump are ion evaporated can be drawn from the Iribarne−Thomson rate law combined with Born's model calculations of the activation energy required for an ion to escape from the liquid. The ionization probability f_i of a certain cluster is proportional to its surface concentration times the exponential of minus the activation energy required for ion evaporation ΔG_i over the thermal energy kT. Although it is clear that surface ion concentration plays an important role (particularly in the case of surfactants), we will to a first approximation ignore it and focus on the exponential term:

$$f_i \sim \exp(\Delta G_i/kT) \tag{2}$$

Hence, to a first approximation, the currents of the various clusters are determined by their activation energies, and one particular ion will dominate the mass spectrum if its activation energy is smaller than that of all the others by several times kT. The Born model treats the ejected cluster ion as a macroscopic drop with given density ρ, radius R, dielectric constant ϵ, and surface tension γ, and determines the energy change associated to moving it from the liquid into the vacuum. This energy has an electrostatic component $q^2(1 - 1/\epsilon)/(8\pi\epsilon_o R)$ and a surface term $4\pi\gamma R^2$ (ϵ_o is the electrical permittivity of vacuum). The sum of both is minimized at a characteristic cluster radius

$$R^{*3} = q^2(1 - 1/\epsilon)/[8^2\pi^2\gamma\epsilon_o] \tag{3}$$

where it takes the value

$$\Delta G^* = [3/(4\pi^{1/3})]q^{4/3}(1 - \epsilon^{-1})^{2/3}\gamma^{1/3}\epsilon_o{}^{-2/3} \tag{4}$$

The critical volume associated to condition (3) is

$$v^* = q^2(1 - 1/\epsilon)/[48\pi\gamma\epsilon_o] \tag{5}$$

For small ions the radius can be controlled by attachment of solvent molecules, and the solvation level typically observed varies qualitatively with q and γ, as predicted in (5). The large ions used in this work tend to be unsolvated, but their radius can still be controlled by clustering. In this case γ would not be the solvent's surface tension, but that of the cluster. Given that there is a critical cluster volume at which ΔG is minimized, it follows that there is a corresponding most favored level of clustering, as observed. Such a critical volume exists for each charge state and increases in Born's model quadratically with z. It hence makes sense that each of the charge states observed would be represented principally at a certain degree of clustering, with intensities decaying rapidly to its right and left. From the mobilities at the maximum peak height we can infer the corresponding radii, as compiled in Table 3 for $z = 1$ and $z = 2$.

These radii are about 0.4 and 0.75 nm for singly and doubly charged ions, respectively, for all solutions except TBAPOS.

4. Conclusions

Acetonitrile solutions of five large room temperature molten salts have been electrosprayed and their mobility spectra used to infer the abundance of the singly and doubly charged clusters formed. Both charge states tend to form in two distinct groups, revealing the existence of two distinct ionization mechanisms. The smallest ions are attributed to ion evaporation, and the larger ones to Dole's charged residue mechanism. This interpretation is reinforced by several other observations made, including the dependence of the mobility spectra on the flow rate of electrosprayed liquid, and the greater sharpness of the peaks from evaporated ions relative to the charged residues. It is also entirely consistent with what would be expected theoretically for evaporating ions, where each charge state would tend to appear dominantly at a certain clustering level.

Although the observations assembled support persuasively our interpretation, a more complete proof would require isolation of the two mechanisms. This has been attempted previously by use of concentrated solutions producing initially very small drops that reached the ion-evaporation limit prior to undergoing a first Coulombic explosion. As a result, the charge residue mechanism could only produce very large clusters, whereas ion evaporation remained effective. We have already noted that, in the case of tetraheptylammonium clusters, this led to the conclusion that ion evaporation takes place up to the cluster $A^+(AB)_4$.[7a] Although this was not originally observed, we note here the presence also of the metastable peaks later interpreted as doubly charged in the "pure ion evaporation" spectra just quoted (Figure 11 of ref 7a). These data leave therefore little doubt about the ion evaporation origin of the first hump, both, for the singly and the doubly charged series.

The new ability to distinguish between ions produced by either mechanism enables making rather interesting new inferences, including the striking fact that clusters involving more than one cation can evaporate directly from charged drops. We also provide data on the mobility in air for a wide range of large clusters, some having masses up to 10 kDalton.

Acknowledgment. This work was supported by NSF grant CTS-9871885, AFOSR grant F-49620-01-1-1416, a gift from Rohm-Haas, and the Postdoctoral Fellowship Program of Korea Science and Engineering Foundation (KOSEF). Helpful discussions with Mr. Ignacio Romero-Sanz and the help of Mr. Sven Ude in the experiments are much appreciated.

References and Notes

(1) Fenn, J. B.; Mann, M.; Meng, C. K.; Wong, S. F.; Whitehouse, C. *Science* **1989**, *246*, 64.

(2) Meng, C. K.; Fenn, J. B. *Org. Mass Spectrom*. **1991**, *26*, 542.

(3) Meng, C. K. Multiple and fractional charging of solute molecules in electrospray ionization. Ph.D. Thesis: Yale University, 1988.

(4) Anacleto, J. F.; Pleasance, S.; Boyd, R. K. *Org. Mass Spectrom*. **1992**, *27*, 660.

(5) Saucy, D.; Ude, S.; Lenggoro, W.; Fernandez de la Mora, J. *Anal. Chem*. **2004**, *76*, 1045.

(6) Loscertales, I. G.; Fernandez de la Mora, J. *J. Chem. Phys.* **1995**, *103*, 5041.

(7) Gamero-Castaño, M.; Fernandez de la Mora, J. *Anal. Chim. Acta* **2000**, *406*, 67. Gamero-Castaño, M.; Fernandez de la Mora, J. *Anal. Chem.* **2000**, *72*, 1426.

(8) Iribarne, J. V.; Thomson, B. A. *J. Chem. Phys*. **1976**, *64*, 2287−2294. Thomson, B. A.; Iribarne, J. V. *J. Chem. Phys.* **1979**, *71*, 4451. Thomson, B. A.; Iribarne, J. V.; Dziedzic, P. J. *Anal. Chem*. **1982**, *54*, 2219.

(9) Kebarle, P.; Peschke, M. *Anal. Chim. Acta* **2000**, *406*, 11.

(10) Dole, M.; Mach, L. L.; Hines, R. L.; Mobley, R. C.; Ferguson, L. P.; Alice, M. B. *J. Chem. Phys*. **1968**, *49*, 2240. Mach, L. L.; Kralik, P.; Rheude, A.; Dole, M. *J. Chem. Phys*. **1970**, *52*, 4977.

(11) Cook, K. D. *Mass Spectrosc. Rev*. **1986**, *5*, 467.

(12) Gamero-Castaño, M.; Fernandez de la Mora, J. *J. Chem. Phys*. **2000**, *113*, 815.

(13) Gamero-Castaño, M.; Hruby, V. *J. Propulsion Power* **2001**, *17*, 977.

(14) Bocanegra, R.; Fernandez de la Mora, J.; Gamero-Castaño, M. *J. Propul. Power* **2004**, *20*, 728.

(15) Romero-Sanz, I.; Fernandez de la Mora, J.; Gamero-Castaño, M. *J. Appl. Phys*. **2003**, *94*, 3599.

(16) Wilkes, J. S. *Green Chem.* **2002**, *4*, 73, and references therein.

(17) Fernandez de la Mora, J. *Anal. Chim. Acta* **2000**, *406*, 93.

(18) Fenn, J. B.; Rosell, J.; Meng, C. K. *J. Am. Soc. Mass Spectrom*. **1997**, *8*, 1147.

(19) Kaufman, S. L. *Anal. Chim. Acta* **2000**, *406*, 3.

(20) Knutson, E. O.; Whitby, K. T. *J. Aerosol Sci.* **1975**, *6*, 443.

(21) Eichler, T. A Differential Mobility analyzer for ions and nanoparticles: Laminar flow at high Reynolds numbers. Senior Graduation Thesis, Fachhochschule Offenburg, Germany, 1997. Herrmann, W.; Eichler, T.; Bernardo, N.; Fernandez de la Mora, J. Turbulent transition arises at Reynolds number 35,000 in a short Vienna type DMA with a large laminarization inlet. Abstract to the annual conference of the AAAR, St Louis, Missouri, October 2000.

(22) Fernandez de la Mora, J.; de Juan, L.; Eichler, T.; Rosell, J. *Trends Anal. Chem.* **1998**, *17*, 328.

(23) Fernandez de la Mora, J.; Thomson, B.; Gamero-Castaño, M. Submitted to *J. Am. Soc. Mass Spectrom.*

(24) Guevremont, R.; Siu, K. W. M.; Wang, J.; Ding, L. *Anal. Chem*. **1997**, *69*, 3959.

(25) Tammet, H. *J. Aerosol Sci*. **1995**, *26*, 459.

(26) Fernandez de la Mora, J.; Loscertales, I. G. *J. Fluid Mech*. **1994**, *260*, 155.